

Test of an Optical Transition Radiation Detector for High-Intensity Proton Beams at FNAL

Victor E. Scarpine, Alex H. Lumpkin, Warren Schappert, Gianni R. Tassotto

Abstract—Initial results are presented of a prototype optical transition radiation (OTR) detector under development at Fermi National Accelerator Laboratory (FNAL). The purpose of this prototype detector is to evaluate the feasibility of using OTR imaging of proton (or antiproton) beams in transport lines for beam position and shape measurements. A secondary purpose is to develop experience in designing, constructing and operating a camera and optics system in high radiation environments. Measurements are made of 120 GeV proton beams with up to 4.7×10^{12} particle intensities. Data are presented of OTR with titanium and aluminum foils.

I. INTRODUCTION

PARTICLE-BEAM diagnostic techniques based on optical transition radiation (OTR) have been demonstrated at a number of facilities over a wide range of beam energy (or Lorentz factor, γ) [1] – [3]. FNAL is pursuing a number of projects where either beam luminosity for the Tevatron collider (Run II) or proton intensity for neutrino experiments requires careful tracking of beam properties, such as transverse profile and shape (tilt), transverse position, emittance and intensity, throughout the facility. The feasibility of using OTR imaging for the relatively low Lorentz factor ($\gamma \sim 129$) intense proton beams at FNAL is based on a comparison with high Lorentz factor electron-beam results at the Advanced Photon Source (APS) linac [3] and proton-beam results at CERN [2]. This comparison suggests that significant levels of OTR will be generated by the generally lower Lorentz factor but higher intensity ($\sim 4.5 \times 10^{12}$ particles) proton beams at FNAL [4].

Optical transition radiation is generated when a charged particle transits the interface of two media with different dielectric constants (e.g., vacuum to dielectric or vice versa) [2, 5]. The effect is a surface phenomenon that can be understood as the collapsing of the electric dipole formed by the approaching beam charge and its image charge in the

dielectric at the surface. As the fields readjust, a pulse of radiation is emitted. Imaging techniques are used to acquire the emitted OTR signal and then reconstruct beam size and position at the dielectric. The expression for the single-particle spectral angular distribution of the number of photons, N , per unit frequency (ω) and solid angle ($d\Omega$) is given by [5, 6],

$$\frac{d^2 N}{d\omega d\Omega} = \frac{2e^2}{\pi \hbar c \omega} \frac{(\theta_x^2 + \theta_y^2)}{(\gamma^{-2} + \theta_x^2 + \theta_y^2)^2}$$

where e is the electron charge, \hbar is Planck's constant, c is the speed of light, γ is the Lorentz factor of the charged particle, and θ_x and θ_y are the angles from the OTR emission axis. For the forward OTR this axis is the same as the particle beam while for the backward OTR this axis is the specular reflection axis. In addition, the intensity of the backward OTR is proportional to the reflectivity of the surface. This expression shows that the angular distribution is maximum at $\theta \sim 1/\gamma$.

Since OTR is a surface phenomenon, thin foils are used as the converter to reduce beam scattering and minimize heat deposition.

II. PROTOTYPE OTR DETECTOR

We have constructed and installed a prototype OTR detector at FNAL. The prototype is located in an air gap located in the AP1 transport line upstream of the antiproton production target. This beamline transports 120 GeV protons with up to 4.7×10^{12} particles in a $1.6 \mu\text{s}$ spill at a rate of one spill every 2 seconds. At this location the rms transverse beam size is ~ 1 mm and $1/\gamma$ is ~ 8 milliradians. In addition, the two titanium vacuum windows on either end of the air gap establish the survivability of foils at this location.

The detector uses either a $12 \mu\text{m}$ titanium or $20 \mu\text{m}$ aluminum foil in the air gap at 45° to the beam that serves as the OTR generator screen. The foil mount has the ability to tilt in order to match the OTR specular reflection axis to the detector optical axis. A lens system collects the OTR generated in a cone of radius $2/\gamma$ about the optical axis and focuses it on to a Charge Injection Device (CID) camera. The CID camera is a standard RS-170 format and operates at 30 image frames per second. The camera is mounted on a translation stage that allows for focus adjustment. The optics operates at a magnification of $1/9$ and produces an equivalent pixel size of approximately $100 \mu\text{m}$ by $100 \mu\text{m}$ at the foil or an 80 mm by

Manuscript received October 29, 2003. This work was supported by the U.S. Department of Energy under contract No. DE-AC02-76CH03000.

V. E. Scarpine is with Fermi National Accelerator Laboratory, Batavia, IL 60510 USA (telephone: 630-840-2571, e-mail: scarpine@fnal.gov).

A. H. Lumpkin is with Argonne National Laboratory, Argonne, IL 60439 USA (e-mail: lumpkin@aps.anl.gov).

W. Schappert was with Fermi National Accelerator Laboratory, Batavia, IL 60510 USA. He is now with Array Systems Computing Inc., Toronto, Ontario, Canada (e-mail: warren@array.ca).

G. R. Tassotto is with Fermi National Accelerator Laboratory, Batavia, IL 60510 USA (e-mail: tassotto@fnal.gov).

55 mm field of view. To maintain focus over the foil, the camera is mounted at an angle to satisfy the Scheimpflug condition. Images of OTR are acquired and saved to a computer using a standard frame grabber card. Camera light levels are controlled by the use of selectable neutral density filters. Figure 1 shows a block diagram of the prototype OTR detector system. For operational purposes, the entire OTR detector can be moved out of the AP-1 transfer line. Foil, camera and detector motions are controlled remotely via a control box or computer.

The multiple titanium vacuum foils at this location produce a high radiation environment. Because of this radiation, the camera and optics are placed approximately one meter from the OTR foil. At this location, the CID camera and optics receive ~ 6 kRad/week. The CID camera has been shown to operate beyond a total dose over 1 MRad [7].

Both aluminum and titanium foils are tested since each as distinct advantages. Aluminum has a higher reflection coefficient but titanium is stronger and has a higher melting point. For future OTR detectors, choice of foil material depends of beam intensity and beam size.

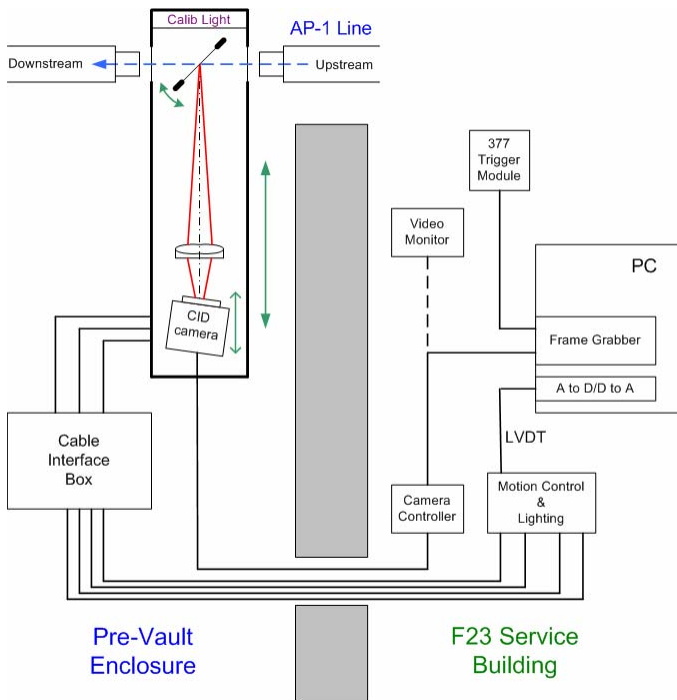


Fig. 1. A block diagram of the prototype OTR detector system.

III. OPTICAL CALIBRATION

We have integrated a simple optical calibration system into the prototype OTR detector to measure image scale and focus. Fiducial holes are placed at precise locations in the foil near the corners of field of view. These holes are then back illuminated and imaged. Images over a range of camera position allow best focus to be determined. Figure 2 shows a

false-color image of the fiducial holes at nominal focus. Image calibration gives an X scale of $123 \mu\text{m}$ per image pixel and a Y scale of $106 \mu\text{m}$ per image pixel.

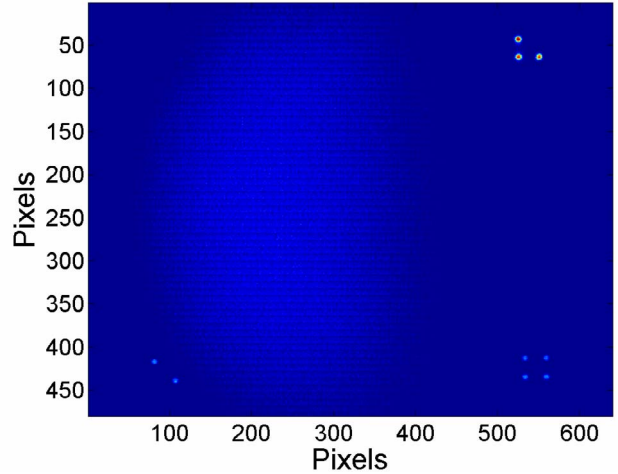


Fig. 2. False-color image of fiducial holes in $12 \mu\text{m}$ titanium foil. The location of fiducials allows the image scale to be determined while fiducial sharpness allows best focus to be determined.

IV. OTR BEAM IMAGES

Measurements have been made of OTR signal generated by 120 GeV proton beams for both titanium and aluminum foils up to an intensity of 4.7×10^{12} particles. Initial images taken with no light attenuation saturate the CID camera so some degree of light attenuation is required. All OTR images presented here have been filtered with a 5×5 median filter to reduce noise artifacts. Also, all of the OTR images are false-color and are therefore normalized.

A. OTR Measurement with Titanium

Figure 3 shows a false-color backward OTR image from 4.5×10^{12} 120 GeV protons through $12 \mu\text{m}$ titanium. Optical transition radiation is attenuated by a factor of 200 in order to avoid camera pixel saturation. This image shows a clear indication that the transverse beam shape is tilted at this location in the AP-1 transfer line. Figure 4 shows vertical and horizontal line profiles of light intensity.

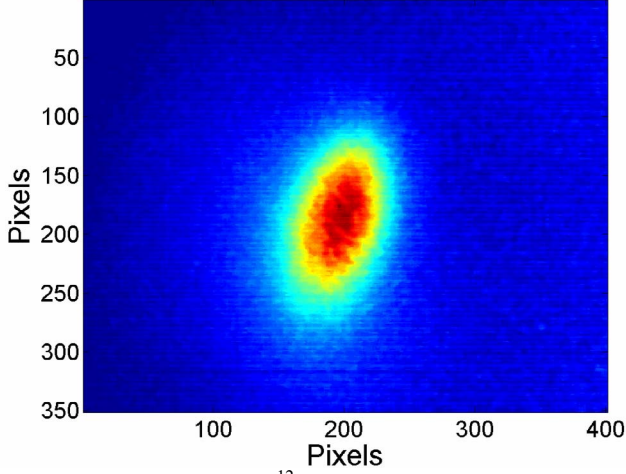


Fig. 3. OTR from 4.5×10^{12} 120 GeV protons through 12 μm titanium foil. Light intensity is attenuated by a factor of 200 to avoid camera saturation.

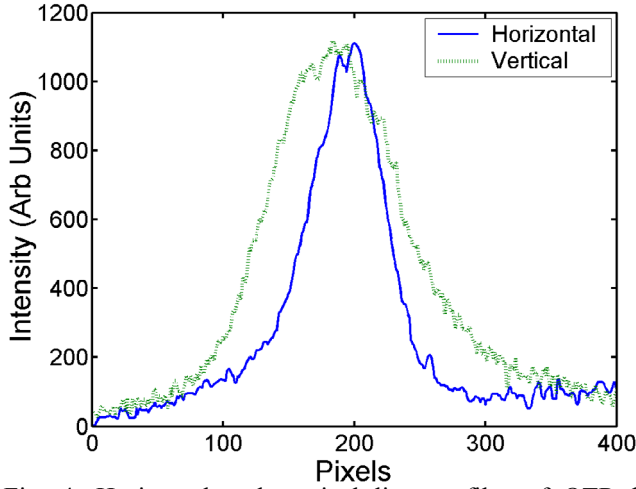


Fig. 4. Horizontal and vertical line profiles of OTR light intensity taken through the maximum of the OTR distribution.

B. OTR Shape Measurement

Figure 5 shows a false-color backward OTR image for 120 GeV protons through 12 μm titanium for a nominal beam size. Figure 6 shows a similar beam where the vertical size has been reduced by a factor of ~ 2 . For both figures the OTR light has been attenuated by a factor of 200. These figures show that the prototype detector tracks the change in beam shape.

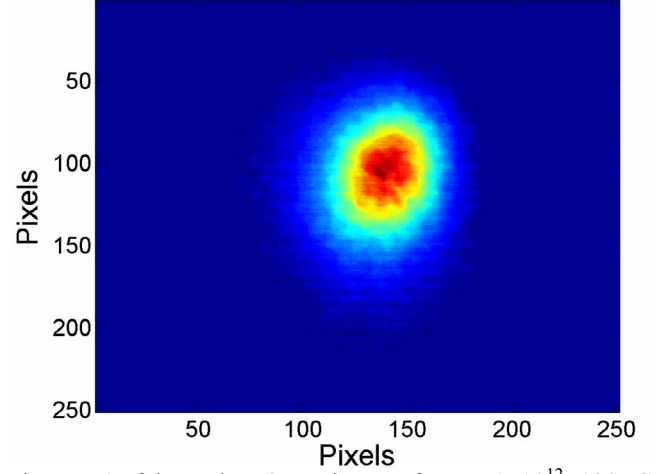


Fig. 5. A false-color OTR image from $\sim 1 \times 10^{12}$ 120 GeV protons through 12 μm titanium foil at nominal beam size.

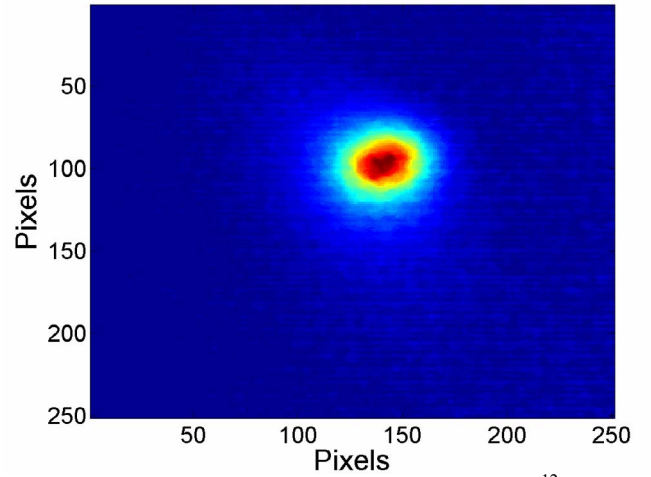


Fig. 6. A false-color OTR image from $\sim 1 \times 10^{12}$ 120 GeV protons through 12 μm titanium foil with a factor of ~ 2 reduction in vertical beam size.

C. OTR Position Measurement

Figure 7 shows OTR images taken with three different vertical beam positions for different spills. The images are of 1×10^{12} 120 GeV protons through 12 μm titanium. The images clearly track the change in beam position and measure a beam position of +11.1 mm and -11.1 mm from nominal center beam position.

The left and center images in figure 7 have similar beam size and shape while the right image appears to have a different beam shape. It is not clear if this is a real beam effect or a shape induced by the titanium foil. Further measurements are needed to understand this effect.

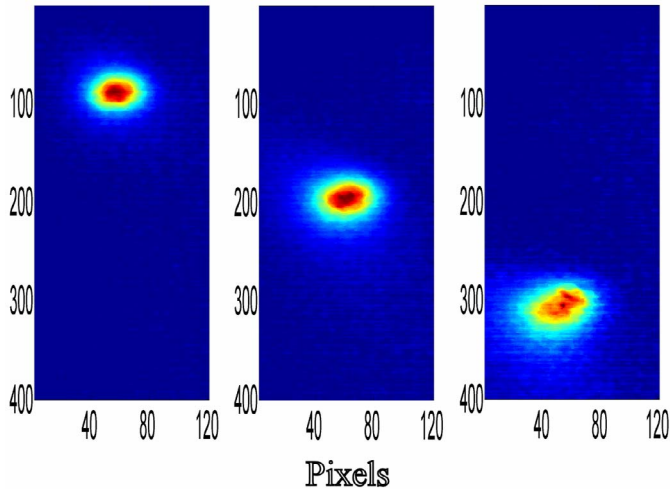


Fig. 7. False-color OTR images from $\sim 1 \times 10^{12}$ 120 GeV protons through 12 μm titanium for different beam positions. The center image is taken at nominal beam position. The left image is taken at +10 mm vertical displacement from nominal and the right image is taken at -10 mm vertical displacement as measured by beam position monitors.

D. OTR Measurement with Aluminum

Figure 8 shows a false-color backward OTR image from 4.7×10^{12} 120 GeV protons through 20 μm aluminum with a factor of 1000 light attenuation. As described above, backward OTR is proportional to the reflectivity of the foil and aluminum has a higher reflectivity than titanium. A factor of 1000 light attenuation for aluminum versus 200 for titanium shows that we are seeing more OTR from the aluminum foil. In addition, similar OTR size and shape from titanium (Fig. 3) and aluminum (Fig. 8), for similar beam conditions, indicate that the foils are not introducing artifacts into the image.

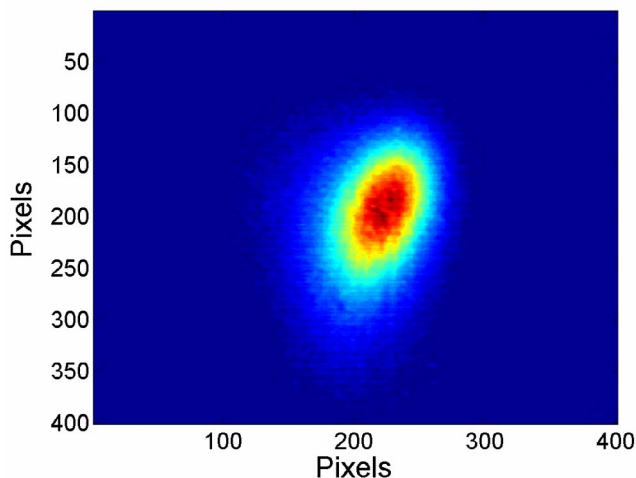


Fig. 8. OTR from 4.7×10^{12} 120 GeV protons through 20 μm aluminum foil with a factor of 1000 light attenuation.

V. SUMMARY

We have developed and installed a prototype OTR detector and have taken first images with 12 μm titanium and 20 μm aluminum foils. Measurements indicate that OTR light levels are strong enough to allow imaging at particle intensities as low as 5×10^9 120 GeV protons for a beam size of ~ 1 mm rms or smaller. Larger beam sizes can be imaged with proportionally higher beam intensities.

Examination of the titanium foil after $\sim 7 \times 10^{17}$ 120 GeV protons shows no surface changes but long-term damage to foils, camera and optics have not been measured.

Optical transition radiation images from this prototype detector suggest that OTR detectors can be used for high-intensity proton beams. Possible OTR applications for FNAL include developing (1) a three-foil beta function matching station in each of the transport lines between the Main Injector and the Tevatron to measure both protons and antiprotons, (2) a beam profiling station for the high-intensity 120 GeV transport lines for NuMI, (3) a beam profiling station for the 8 GeV transport lines, (4) a beam halo detector, (5) a single bunch detector with a gated, intensified camera and (6) an OTR foil for use in the Tevatron for injection studies.

VI. ACKNOWLEDGMENT

We thank our colleagues in the FNAL Beams Division for their contributions to the development, integration and testing of our prototype OTR detector: Eugene Lorman, Jim Morgan, Tony Leveling and Elvin Harms. In addition, we wish to thank Carl Lindenmeyer, John Korieneck, Ron Miksa, Karen Kephart and Wanda Newby of FNAL Particle Physics Division for their outstanding work in the mechanical design and construction of the detector. The authors also acknowledge the support of Gianfranco Ferioli (CERN) for conversations on OTR detectors. We would also like to thank Stephen Pordes (FNAL) and Bob Webber (FNAL) for their enthusiasm and encouragement for pursuing OTR detectors.

VII. REFERENCES

- [1] P. Goldsmith, J. V. Jelley, *Phil. Mag.*, 4, 836 (1959).
- [2] J. Bossert, J. Mann, G. Ferioli, L. Wartski, "Optical Transition Radiation Proton Beam Profile Monitor," CERN/SPS 84-17.
- [3] A. H. Lumpkin et al., *Nucl. Instr. and Methods*, A429, 336 (1999).
- [4] A. H. Lumpkin, V. Scarpine, "The Feasibility of OTR Imaging of High-Intensity Proton Beams at FNAL," Submitted to Particle Accelerator Conference, May 12-16, 2003.
- [5] L. Wartski, J. Marcou, S. Roland, *IEEE Trans. on Nucl. Sci.*, Vol. 20, No. 3, June 1973.
- [6] D. W. Rule et al., "The Effect of Detector Bandwidth on Microbunch Length Measurements made with Coherent Transition Radiation," *Advanced Accelerator Concepts: Eighth Workshop*, W. Lawson, C. Bellamy, and D. Brosius, eds., AIP 472, p.745-754, 1999.
- [7] J. Carbone, J. Zarnowski, M. Pace, S. Czebiniak, R. Carta, "Megarad and Scientific CIDs," *Proceedings of SPIE*, Vol. 2654, p.131-138, 1996.